Numerical Investigation of the Hygrothermal Behaviour of a Hemp-Concrete Room: Hysteresis Effect of the Sorption Isotherm and its Temperature Dependency

Georges Costantine[1], Chadi Maalouf[1], Elias Kinab[2], Guillaume Polidori[1]
Georges.Costantine@univ-reims.fr, Chadi.Maalouf@univ-reims.fr, Elias.Kinab@ul.edu.lb, Guillaume.Polidori@univ-reims.fr
[1]Thermomechanical Laboratory LTM, GRESPI, SFR Condorcet FR CNRS 3417, University of Reims-Champagne-Ardenne, 51 687, Reims, France
[2]Lebanese University, Faculty of Engineering, Section II, Roumieh, Lebanon

Abstract

Building sector energy consumption is growing with the world's development and its occupants' wellbeing requirements. One of the solutions to reduce its energy costs is the use of bio-based materials as thermal insulation materials, recommended for their low environmental impacts. In this context, hemp concrete became very popular in the field of constructions. However, rare are the studies about the modelling of hemp concrete hygrothermal behaviour at the room scale, which presents the purpose of this work. The effects of hysteresis and temperature dependency of sorption isotherms are investigated in a numerical model of a hemp concrete wall coupled to a room and taking into account different ventilation strategies.

Introduction

According to the most recent studies, buildings are worldwide known as the most energy and resources consuming sector: actually, as mentioned in the French Thermal Regulations of 2012 and in the United Nations Environmental Program of 2016 (UNEP), buildings are responsible of almost 43 % and 40 % of the total energy and global resources consumption respectively. In front of these dangerous challenges, and in a context of promoting energy efficiency, seeking alternatives has become very urgent. Therefore, building sector has undergone a notable evolution towards innovative construction materials (D'Alessandro et al. 2014) (Asdrubali et al. 2015), conventionally called "green" materials, which have proved their ability to act as eco-friendly products.

Hemp concrete, marked in the commercial field under the name of hempcrete, is one of these famous vegetal fibre materials. Obtained by mixing hemp shives to a mineral binder (the lime), water and some additives, hempcrete was subject to several studies, at the material and wall scales, and its experimental characterization is almost complete (Collet 2004)(Cerezo 2005)(Elfordy et al. 2008). Recent works have shown also the importance of including hysteresis effect in modelling its hygrothermal behaviour to assess relative humidity profiles within the walls (Lelievre et al. 2014) (Y. Ait Ouméziane 2013). However, there are no works about this impact on the hempcrete room scale modelling.

This work aims to carry out a study of the hemp concrete at the room scale, with taking into account the hysteresis phenomenon. The sorption curves dependency on the temperature variations is also studied. The model is developed and validated under SPARK simulation tool (Tran Le et al. 2010) and then applied to hemp concrete wall façade coupled to a room, used as a commercial office. Simulations are run for two strategies of ventilation: constant air flowrate and relative humidity sensitive flowrate.

Numerical study

Mathematical models

Coupled heat and moisture transfer models for a simple layer building materials are studied in several researches: Künzel (1995) developed a model in which moisture transfer is due to relative humidity and temperature gradients. In 1997, Mendes et al. (Mendes et al. 1999) showed a model based on Philip and De Vries (1957) theory, with similar assumptions as Künzel, but this time moisture transfer is governed by volumetric moisture content gradient. Thus, Umidus model (Mendes et al. 1999) is created : both diffusion and capillary regimes are taken into account and the water transfer in the vapor and liquid phases through the material can be analysed for any type of climate. Moreover, in 1989, Keresteciogl and Gu (1989) investigated the phenomenon using the evaporation-condensation theory in unsaturated liquid flow stage. In addition, Burch and Thomas (Burch and Thomas 1991) developed a computational model using finite-difference method able to estimate heat and mass transfers through composite walls under non-isothermal conditions. Moreover, the model of Ozaki et al. (2001) takes into account the moisture transfers in both liquid and vapor phases coupled to the heat generated by the phase change due to the moisture sorption process. Recently, Oumeziane (2013) used a model to describe heat and moisture transfers in hemp concrete based on Philip and De Vries approach and takes into consideration the effects of the temperature-dependency of the sorption curves on the numerical model.

In this study, Umidus model, where moisture is transported under liquid and vapour phases, is used. The mass conservation equation is then:

$$\frac{\partial \theta}{\partial t} = \frac{\partial}{\partial x}\left(D_T \frac{\partial T}{\partial x}\right) + \frac{\partial}{\partial x}\left(D_\theta \frac{\partial \theta}{\partial x}\right) \qquad (1)$$

With the following boundary conditions (x = 0 and x = L):

$$-\rho_l\left(D_T\frac{\partial T}{\partial x}+D_\theta\frac{\partial\theta}{\partial x}\right)\Big|_{x=0,e}=h_{M,e}\left(\rho_{v,a,e}-\rho_{v,s,e}\right) \quad (2)$$

$$-\rho_l\left(D_T\frac{\partial T}{\partial x}+D_\theta\frac{\partial\theta}{\partial x}\right)\Big|_{x=L,i}=h_{M,i}\left(\rho_{v,s,i}-\rho_{v,a,i}\right) \quad (3)$$

"*e*" and "*i*" represent respectively the outside and inside, "*s*" refers to the wall surface, and "*a*" to the ambient air. $D_T=D_{Tl}+D_{Tv}$ and $D_\theta=D_{\theta l}+D_{\theta v}$, where D_{Tl} is the liquid phase transport coefficient associated to a temperature gradient, D_{Tv}, the vapor phase transport coefficient associated to a temperature gradient, $D_{\theta l}$, the liquid phase transport coefficient associated to a moisture content gradient, $D_{\theta v}$, the vapor phase transport coefficient associated to a moisture content gradient, D_T, the mass transport coefficient associated to a temperature gradient and D_θ, the mass transport coefficient associated to a moisture gradient (Crausse et al. 1996).

$$D_\theta=\frac{\delta_a}{\mu}\frac{P_{vs}}{\rho_0}\frac{1}{\xi} \quad (4)$$

Vapour transport coefficient under a temperature gradient is given by the relation:

$$D_{T,v}=\phi\frac{\delta_a}{\rho_l\mu}\frac{dP_{vs}}{dT} \quad (5)$$

D_{θ_v} is expressed as follows:

$$D_{\theta v}=\frac{D_{Tv}\times P_{sat}}{\xi\left(\emptyset\times\frac{dP_{vs}}{dT}+P_{sat}\times\frac{1}{\xi}\times\xi_T\right)} \quad (6)$$

One dimensional model of the energy conservation equation with coupled temperature and moisture for a porous media is considered, and the effect of the absorption or desorption heat is added. This equation is written as:

$$\rho_0\,Cp_m\frac{\partial T}{\partial t}=\frac{\partial}{\partial x}\left(\lambda(T,\theta)\frac{\partial T}{\partial x}\right)+L_v\rho_l\left(\frac{\partial}{\partial x}\left(D_{T,v}\frac{\partial T}{\partial x}\right)+\frac{\partial}{\partial x}\left(D_{\theta,v}\frac{\partial\theta}{\partial x}\right)\right) \quad (7)$$

$$Cp_m=Cp_0+Cp_l\frac{\rho_l}{\rho_\theta} \quad (8)$$

Where Cp_m is the average specific capacity, which takes into account the dry material specific heat and the contribution of the specific heat of the liquid phase. λ is the thermal conductivity depending on moisture content and the temperature in Kelvin.

Boundary conditions take into account radiation, heat and phase change.

$$-\lambda\frac{\partial T}{\partial x}\Big)_{x=0,e}-L_v\,\rho_l\left(D_{T,v}\frac{\partial T}{\partial x}+D_{\theta,v}\frac{\partial T}{\partial x}\right)_{x=0,e}=h_{T,e}\left(T_{a,e}-T_{s,e}\right)+L_v\,h_{M,e}\left(\rho_{ve,a,e}-\rho_{ve,s,e}\right)+\emptyset_{ray,e} \quad (9)$$

Air model

The net heat transferred into the room across its faces must equal the heat stored in the volume of air in the room. That involves heat fluxes through the envelope (transmission, long and short-wave radiation input), additional thermal loads, air exchange due to natural convection or air conditioning systems and thermal losses due to thermal heat bridges. The energy equation can be written as:

$$\left(\rho_i C_p V+I\right)\frac{\partial T}{\partial t}=\emptyset_{West}-\emptyset_{East}+\emptyset_{South}-\emptyset_{North}+\emptyset_{Bottom}-\emptyset_{Top}+\emptyset_{source} \quad (10)$$

(10)

where *I* is the room thermal inertia and $\emptyset_i$ are the amounts of heat transferred by conduction from adjacent walls or from the outside or from possible sensible heat sources.
The humidity condition in the room is due to moisture transfer from interior surfaces, moisture production rate and the gains or losses due to air infiltration, natural and mechanical ventilation as well as sources or sinks due to the room occupants. This yields to the following mass balance equation for the room's air:

$$V\frac{\partial\rho_a}{\partial t}=Q_{mWest}-Q_{mEast}+Q_{mSouth}-Q_{mNorth}+Q_{mBottom}-Q_{mTop}+Q_{msource} \quad (11)$$

Concerning the radiation exchanges in the room, the mean radiant temperature method (Tran Le 2010) is used to calculate long wave radiations exchange between walls. For the short-wave radiations, it is assumed that radiant energy enters the room by the window and is distributed by the quota of 0.6 for the floor and 0.1 for the other walls.

Review of the hysteresis modelling in the literature

Hysteresis is observed in the sorption curves of hygroscopic building materials, namely the hempcrete. Physically, sorption curves describe the equilibrium between the material water content and the surrounding air relative humidity. The hysteresis phenomenon is due

to the "ink bottle" effect (Collet et al. 2008) which can be explained by the fact that water isn't retained in the materials' pores at the same manner it fulfils them. Litterature provides many models describing the hysteresis phenomenon in porous materials: in fact, three global models can be distinguished: physical models developed by Mualem (1974), mathematical models of Cool and Parker (1987), and emperical models proposed by Pedersen (1990). The first two models are predictive ones and require only main sorption curves to be developed. The emperical ones require at least one main sorption curve to work correctly. New researches done by Steeman (2009) and Van Belleghem (2010) showed that hysteresis influences the moisture transfer in porous materials. Moreover and particularly in hemp concrete, Samri (2008), Tran Le (2010), and Lelievre et al. (2015) have proved the importance of considering the hysteresis phenomenon in global transfer models (heat, air and moisture). Although, studies of multilayered walls including hysteresis remain scarce: Aït Ouméziane (2013) worked to improve the modelling by including hysteresis to the hemp concrete in a multilayered wall and assuming perfect contact between the layers. Similarly, Maděra et al. (2012) took into account the hysteresis in the insulating material of the wall and not within the plasters. Johannesson and Janz (2009) showed that hysteresis could be modelled in all the layers of a multilayered wall. Moreover, Colinart et al. (2016) proved that including the hysteresis in all the layers of a multilayered hemp concrete wall subjected to isothermal and non-isotehrmal conditions leads to a better prediction of the relative humidity within the wall.

Mathematical model for the hysteresis

In this article, the empirical model proposed by Pedersen (1990) to describe the hysteresis occuring in hygroscopic materials like wood is used and adapted for the hemp concrete case. Pedersen's approach is based on the weighted values of the moisture capacity or on the slopes of adsorption and desorption curves described by:

$$\xi_a = \frac{\partial \theta_a}{\partial \varphi} \tag{12}$$

$$\xi_d = \frac{\partial \theta_d}{\partial \varphi} \tag{13}$$

Where θ is the actual volumetric water content (m^3/m^3) for a fixed temperature, φ the relative humidity of the air and a and d represent adsorption and desorption phenomenon respectively. Main adsorption and desorption curves are given in equations (14) and (15):

$$\frac{\theta(\varphi)}{\theta_{max}} = \left(1 - \frac{ln(\varphi)}{A_a}\right)^{\frac{-1}{n_a}} \tag{14}$$

$$\frac{\theta(\varphi)}{\theta_{max}} = \left(1 - \frac{ln(\varphi)}{A_d}\right)^{\frac{-1}{n_d}} \tag{15}$$

The coefficients $\boldsymbol{A_a}$, $\boldsymbol{A_d}$, $\boldsymbol{n_a}$ and $\boldsymbol{n_a}$ are calculated using the least squares method based on the experimental results of sorption curves of Lelievre et al. θ_{max} is the maximum water content. After a series of alternating processes of adsorption and desorption, intermediate scanning curves are modelled by (Rode and Clorius 2004):

$$\xi_{hyst,a} = \frac{\gamma_a(\theta - \theta_a)^2\xi_d + (\theta - \theta_d)^2\xi_a}{(\theta_d - \theta_a)^2} \tag{16}$$

$$\xi_{hyst,d} = \frac{(\theta - \theta_a)^2\xi_d + \gamma_d(\theta - \theta_d)^2\xi_a}{(\theta_d - \theta_a)^2} \tag{17}$$

γ_a and γ_d depend on the type of the material studied. For the case of hemp concrete, they can be fitted based on the experiments of the moisture buffering value of the hemp concrete done by Lelievre et al. according to the NordTest protocol as shown in Figure 1.

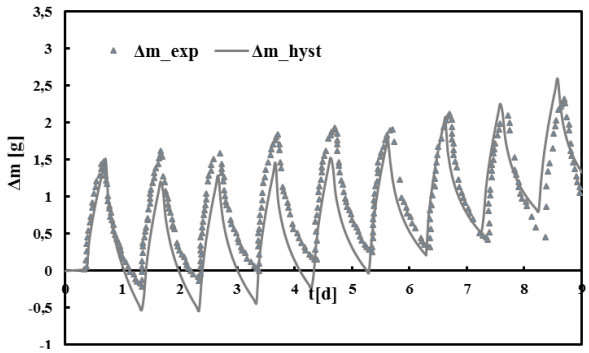

Figure 1: mass variations of hemp concrete specimen during the NordTest experience

Comparing experimental (Δm_exp) and numerical (Δm_hyst) specimen mass variations shows a convergence of the mass during the repeating cycles (adsorption – desorption). The choices of γ_a and γ_d are fixed and adopted in the numerical model including hysteresis.

Sorption curves temperature dependency

The sorption curves temperature dependency of the hemp concrete is considered by allowing several sorption curves to describe sorption characteristics at different temperature levels. So far, the study of the temperature effect on the sorption characteristics for bio-based materials is new. Researches have shown that sorption capacity of materials depends on the temperature: increasing temperature entails that the isosteric moisture content can be reached in equilibrium with a higher relative humidity (Tran Le et al. 2015). Three main reasons can explain this phenomenon (Oumeziane et al. 2016): firstly, the microstructure alteration due to the

temperature (for example, the enlargements of pores can be attributed to a rise of temperature). Secondly, the modification of water thermophysical properties with temperature. And finally, the thermodynamic evolution of sorption mechanism (the exothermic process of adsorption). In the case of hemp concrete, Oumeziane proved the necessity of considering the effect of the temperature in modelling its hygrothermal behavior. Moreover, Rode and Clorius worked on the coupling between temperature and hysteresis effects and proved that an increase of temperature results in a reduction of the hysteresis loop. Poyet and Charles (2009) and Milly (1982) proposed two well known models in the literature. Milly's model is based on the temperature effect on the intrinsic properties of water to establish the sorption curves. The temperature dependent sorption characteristics are expressed as:

$$\varphi_2(T_2,\theta) = \varphi_1(T_1,\theta)\, e^{C_\varphi (T_2 - T_1)} \tag{18}$$

$$C_\varphi = \frac{1}{\varphi}\frac{\partial \varphi}{\partial T} \tag{19}$$

However, Poyet and Charles considered this approach not sufficient to a good prediction of the concrete hygrothermal behavior. Thus, they proposed another model describing the relation between sorption characteristics at different temperatures and based on the differential heat of sorption which can be written as follows:

$$\varphi_2(T_2,\theta) = \varphi_1(T_1,\theta)\frac{P_{sat}(T_1)}{P_{sat}(T_2)}\, e^{q_{st}(\theta)\frac{M_1}{R}\left(\frac{T_2 - T_1}{T_1 T_2}\right)} \tag{20}$$

Where M_1 is the water molar mass (kg.mol^{-1}), R the ideal gas constant (J.mol^{-1}.K^{-1}), and q_{st} the isosteric heat (J.kg^{-1}) calculated from two sorption isotherms at two different temperatures (T_1 and T_2) as shown in Figure 2.

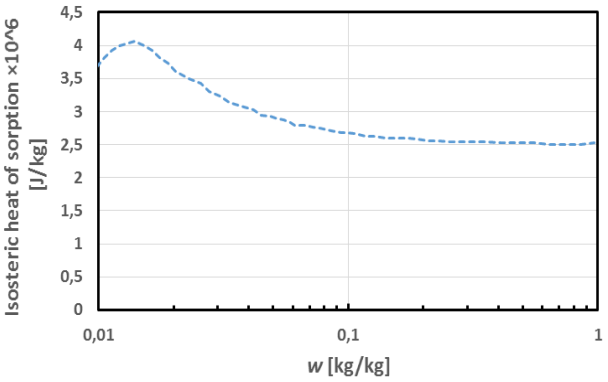

Figure 2: Isosteric heat of sorption (Poyet and Charles Model)

Poyet and Charles' approach is used in the numerical model. Using relation (20), main sorption curves are computed and implemented in SPARK respecting the form of equations (14) and (15), where $\boldsymbol{n}$ is a constant calibrated on the average sorption curve between main adsorption and desorption curves, $\boldsymbol{\theta_{max}}$ a linear function of the temperature, and $\boldsymbol{A_a} = \boldsymbol{A_d} = \boldsymbol{A}$ with $\boldsymbol{A}$ a linear function of the temperature as well. Figure 3 gives a 3D representation ($\boldsymbol{\varphi}$,$\boldsymbol{\theta}$, and $\mathbf{T}$) of the sorption curves.

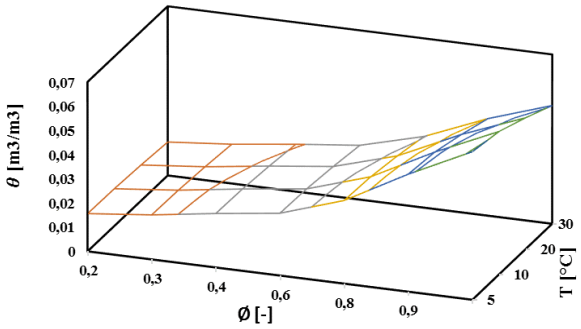

Figure 3: 3D representation of sorption curves

Simulation environment SPARK

In order to solve the previous equation system, the Simulation Problem Analysis and Research Kernel (SPARK) tool is used. Numerical solution is based on the finite difference iterative method. SPARK allows solving efficiently differential equation systems. Each component is represented by an object that contains its appropriate mathematical model. Equations are defined in a generic matter called classes. Model is completed by linking objects together.

Validation of the numerical model on the wall scale

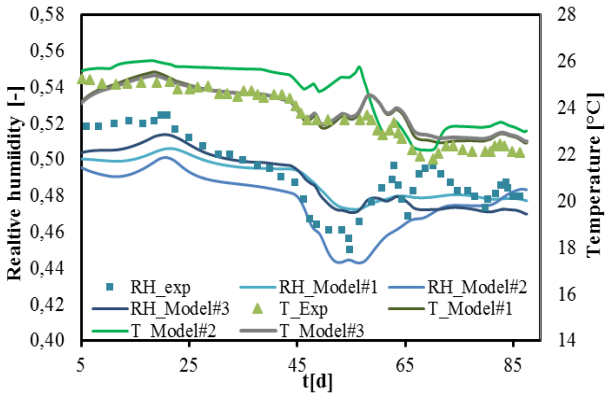

Figure 4: comparison between numerical and experimental temperatures and relative humidities at the wall scale

The numerical model is investigated at the wall scale through a comparison between simulations results and experimental data provided by Lelievre et al. The sample studied is a single layer wall made of 36 cm of hemp concrete, subjected during 87 days to indoor and outdoor conditions for temperature and relative humidity as can be seen in Figure 5. Temperature and relative humidity through the wall are monitored at three different locations using specific sensors. Three types of numerical models are tested and compared. Through this work, they will be labelled by Model#1, Model#2 and Model#3. The characteristics of each model are presented in Table 1.

The results plotted in Figure 4 are only presented for the inner side of the wall.

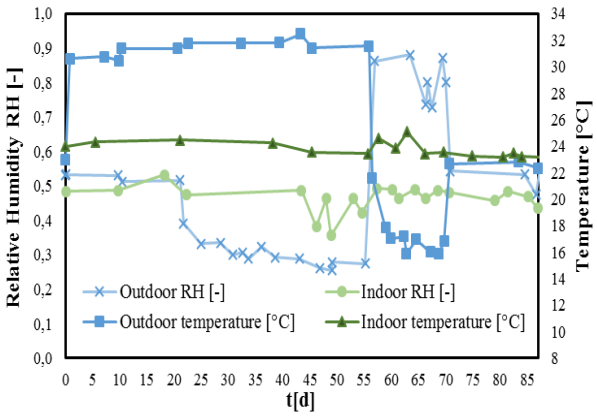

Figure 5: Boundary conditions for the experiment of model validation

Table 1: Characteristics of the numerical models studied

Models	Description
Model#1	▪ Standard model for heat and moisture transfers (simplified model) ▪ Average sorption curve of the hemp concrete is implemented in the model
Model#2	▪ Model for heat and moisture transfers including the hysteresis loop occurring within the hemp concrete and based on Pedersen-Rode approach ▪ Adsorption, desorption and scanning curves are computed and used in the modelling ▪ Initialization of the parameters is taken from the adsorption curve
Model#3	▪ Model for heat and moisture transfers accounting for the temperature dependency of the sorption isotherms and based on Poyet and Charles' approach ▪ The average sorption curve of the hemp concrete is used with variable parameters (function of temperature)

The three models predict very well the temperature and relative humidity at the indoor side of the wall. Effectively, the maximum discrepancies obtained between numerical and experimental results remain less than 4 % for the relative humidity profiles and less than 2 °C for the temperature profiles (taking into consideration a precision of 2% for the humidity sensors and 1 °C for the temperature sensors).The numerical models are therefore validated at the wall scale and will be applied in the study at the room scale.

Case studies

In this study, a virtual office of 24 m^2 and 3 m height is considered. Its South façade (6 × 3 m^2) consists of a simple layer of 36 cm of hemp concrete and contains a double glazing window covering 40 % of its area (7.2 m^2). Properties of the hemp concrete are listed in Table 2. Other vertical walls are multilayers made of 12 cm of cork with internal and external coatings of 1 cm of gypsum. Moisture transport is also considered among these layers with reduced mass coefficients at the surfaces, in order to emphasize the impact of moisture diffusion in the hemp concrete layer on the surroundings. Sources of heat in the room are due to two computers of 130 W each, a LED light of 90 W. The office is supposed to be occupied by two persons for 6 days per week (Monday till Saturday from 8 AM to 13 PM and from 14 PM to 18 PM). Internal temperature is conditioned according to two strategies: from November to April, it is set at 20 °C during occupation period and 17 °C during vacancy time. And for the remaining months, a free floating period allows the temperature fluctuation is allowed to fluctuate between 17 °C and 28 °C. Heating and cooling loads are calculated using a proportional-integrator PI controller.

Table 2: Hemp concrete properties

Properties	Hemp concrete
Thermal conductivity [$W.m^{-1}.K^{-1}$]	λ = 0.00818+0.000276T+0.0024w
Density [$Kg.m^{-3}$]	ρ = 450
Thermal capacity [$J.kg^{-1}.K^{-1}$]	C_p = 1000
Coefficient of resistance to vapor [-]	μ = 5

Concerning the ventilation systems, two different types are tested: first, a constant flow rate of air (36 m^3/h) which takes into account the mechanical ventilation (0.5 vol/h) and the infiltration rate (0.2 vol/h) based on the norm NF EN 12831; second, the relative humidity sensitive rate which depends on the indoor relative humidity of the office as shown in Figure 6.

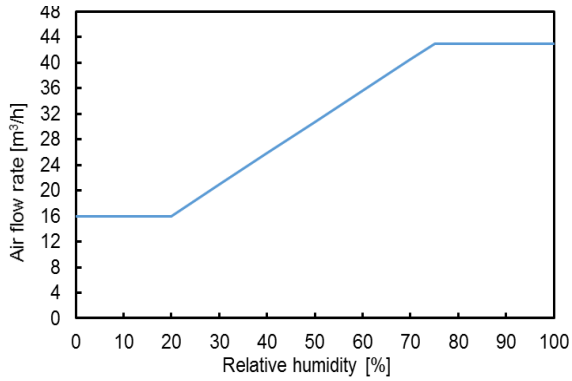

Figure 6: Ventilation air flow rate in the relative humidity sensitive ventilation system

An additional night free cooling of 1.5 vol/h is considered in the summer season (from 3 A.M to 8 A.M) to optimize cooling energy consumption.
Thermal convection coefficients used to calculate convected heat fluxes between indoor air and the ceiling, the floor and the vertical walls are taken from CODYBA software library (Noel 2004) as figured in Table 3.

Table 3: Thermal convection coefficients

	Values [W.m^{-2}.K^{-1}]
External vertical façade	16
Internal floor	1.38
Internal vertical walls	3
Internal ceiling	5.5
Glass	4.5

Mass transfer coefficients are deduced from the thermal ones thanks to Lewis relation as follows:

$$L_e = \frac{h_T}{h_M \rho_a C_{p_a}} \qquad (21)$$

Whereas L_e si the Lewis number, ρ_a and C_{p_a} are respectively the density and the specific heat of the air and h_T and h_M represent the heat and mass convection transfer coefficients.

At the beginning, simulations are run for a whole year . A second annual simulation for each case is also done to insure the initialization of the parameters from the previous simulation. The time step in the modelisation is set to 720 s. The data corresponding to the climate of Nancy city, located in the North East of France, is applied, so that weather conditions including outdoor temperature, relative humidity, solar radiation density as well as sky temperature are introduced as inputs to the models.

Simulation results

Calculation time

The implementation of the models is quite different for each case. Whilst the standard model is relatively easy to be created, modelling the hysteresis requires putting suitable conditions when changing from adsorption to desorption and calculating intermediate moisture capacities. Isotherms temperature dependency involves the determination of variable coefficients of sorption curves with the temperature. It requires also the calculation of a new moisture capacity expression by calculating the average sorption curve derivative with respect to the temperature. The preparation procedure entails calculation time differences in each annual simulation, as shown in Table 4.
Model#2 is the most time-consuming, since at each time step, a test will be done to know if adsorption or desorption is occurring. Model#1 is the fastest one, thanks to its simple equations which facilitate the execution. Model#3 requires more time than Model#1 because of the calculation of sorption curve variable coefficients and isothermal and non-isothermal slopes. Calculation time increases with the relative humidity sensitive flow rate since the air renewal flowrate is calculated in this case for each time step.

Table 4: Calculation time required for each case study

Calculation time	Constant air flow rate	Variable air flow rate
Model#1	1 h 11 min	1 h 18 min
Model#2	6 h 15 min	8 h 15 min
Model#3	1 h 38 min	1 h 50 min

Constant air flow rate case

This section deals with the indoor room conditions during winter and summer for a constant ventilation flowrate. For greater understanding, and since presenting the results for a whole year could not visualize correctly the difference between the models, two periods of 10 days each are depicted in the winter (end of February – beginning of March) and in the summer (September) seasons as shown in Figures (7) till (10).

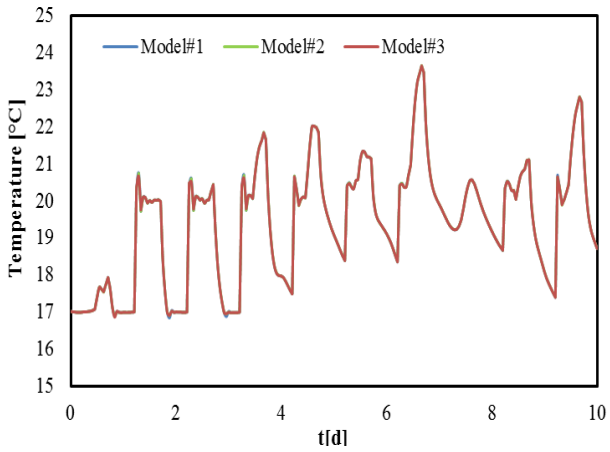

Figure 7: Indoor air temperature during 10 days of the winter season

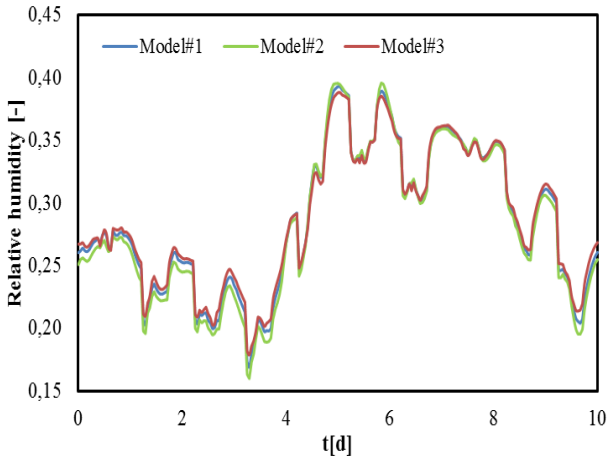

Figure 8: Indoor air relative humidity during 10 days of the winter season

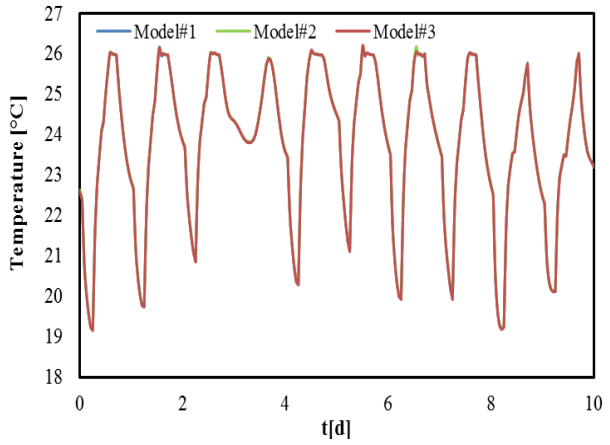

Figure 9: Indoor air temperature during 10 days of the summer season

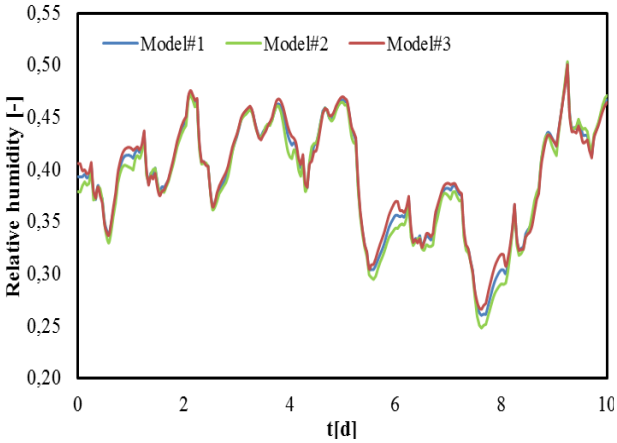

Figure 10: Indoor air relative humidity during 10 days of the summer season

It is obviously detected that the temperature profiles are almost the same for the three models during winter or summer since it is regulated by the PI controller. Indoor air relative humidities are also very close but many observations can be deduced: fisrt, the indoor air relative humidity in the winter varies between 16 % and 40 % while its range in the summer is relatively higher (25 % – 50 %). This is related to the ventilation air which is extracted from the outside at a higher moisture content in the summer due to the increasing in the temperature. Second, the model with hysteresis (Model#2) gives almost the lowest relative humidity (2 to 2.5 % of differences in comparison with the standard model or Model#1), and the model with temperature dependency gives the highest relative humidity especially in the summer (1 % of difference with Model#1 and 1.5 to 2 % with Model#2). This can be explained by the fact that with hysteresis, the wall of hemp concrete retains more moisture because of the "ink bottle" effect, so that indoor air becomes drier. On the other hand, to explain the impact of temperature dependency model, during summer, the wall is subject to a higher temperature which entails a shift of the sorption curve downwards or in other terms, in the moisture content of the wall. Therefore, the hemp concrete becomes drier leading to an increasing of the indoor air humidity.

Annual heating and cooling demands are resumed in Table 5. No strong differences are detected between the three models.

Table 5: Annual heating and cooling energy for the three models in the case of constant ventilation rate

Models	Heating Energy (kWh)	Cooling Energy (kWh)
Model#1	884.49	135.76
Model#2	887.18	138.15
Model#3	891.18	133.42

Maximum heating demand is found for the temperature dependency model with 891.18 kWh, whilst the standard model requires 884.49 kWh and the model with hysteresis needs 887.18 kWh. In fact, with Model#3, the wall is more desorbing moisture on its internal surface. The desorption, being endothermic, absorbs then more heat, causing an elevation in the heating demands in the winter. The difference is less visible with Model#2 because the two phenomena of exothermic adsorption and endothermic desorption occurring within the wall counterbalance each other. For cooling loads, the highest load is observed for the Model #2 with 138.15 kWh, while Model#3 shows a cooling demand of 133.42 kWh. During summer, with the temperature dependency model, high temperatures induce a higher thermal conductivity of the wall since its expression is controlled by the temperature T due to the deacreasing of the water content w. The cooling load decreases because heat is less stored inside the office. Otherwise, with the hysteresis model, lower air relative humidity is a sign of favoured adsorption in the wall. And since it is exothermic, it causes a higher demand for the cooling in the room.

Relative humidity sensitive ventilation case

A similar analysis is conducted for the relative humidity sensitive ventilation rate. Same periods are selected and investigated in Figures (11) until (14).

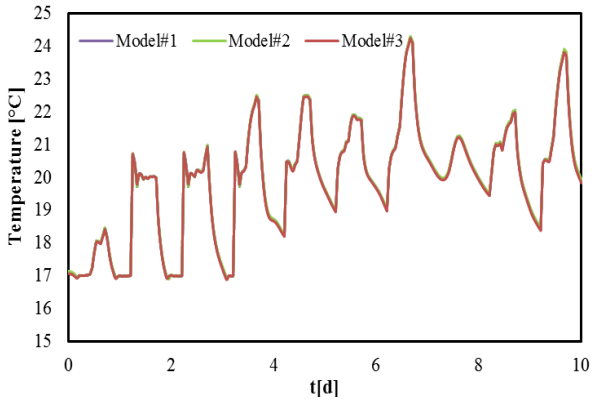

Figure 11: Indoor air temperature during 10 days of the winter season

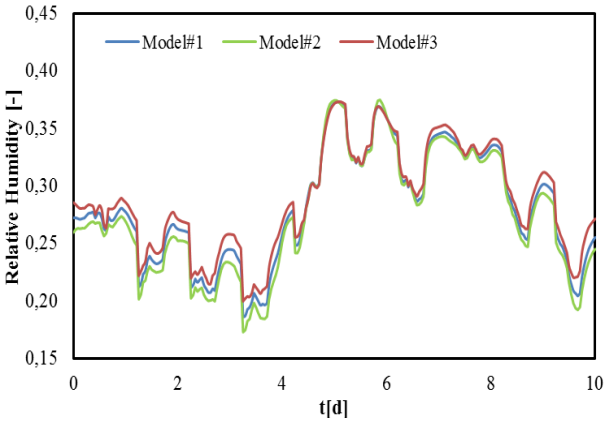

Figure 12: Indoor air relative humidity during 10 days of the winter season

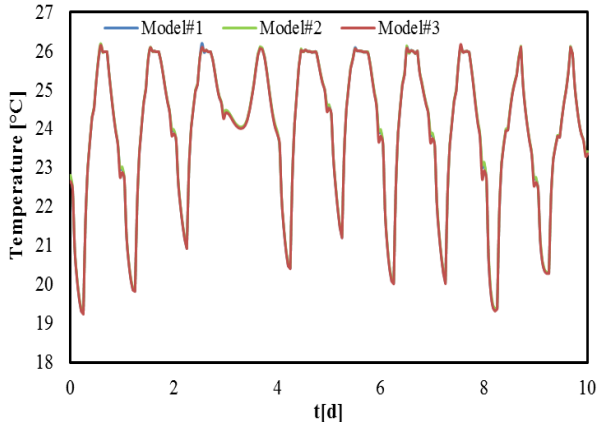

Figure 13: Indoor air temperature during 10 days of the summer season

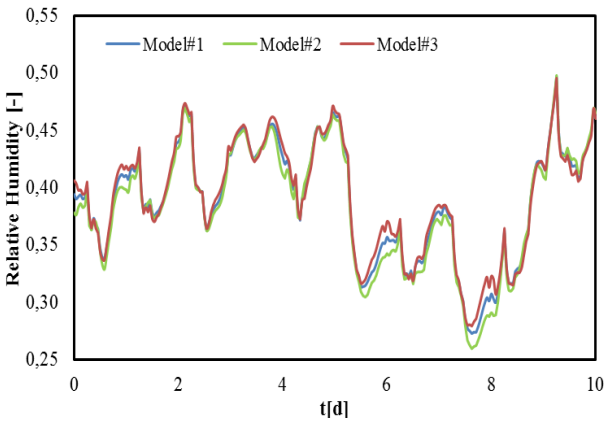

Figure 14: Indoor air temperature during 10 days of the summer season

Same observations are found in the relative humidity sensitive ventilation case. Discrepancies in the indoor relative humidity are slightly more pronounced. On the contrary, as can be seen in Table 6, heating energy demand decreases sharply in this case (32 % lower) with a slight increase in the cooling demand (11 % higher): in fact, during the winter, the indoor relative humidity, being lower than the outdoor, decreases the ventilation air flowrate as well as the heating load. Otherwise, during summer, the indoor relative humidity is higher which enhances the needs for the cooled air.

Table 6: Annual heating and cooling energy for the three models in the case of sensitive ventilation rate

Models	Heating Energy (kWh)	Cooling Energy (kWh)
Model#1	600.85	150.93
Model#2	598.47	154.12
Model#3	608.82	148.22

Small differences appear between the annual energy demands for heating and cooling between the three models. The consumption for cooling during summer is the highest for Model#2 with 154.12 kWh and the lowest for Model#3 with temperature dependency (148.22 kWh) for the same reasons discussed before. In addition, Model#3 shows the highest heating energy (608.82 kWh) whilst the lowest goes for Model#2 (598.47 kWh). With variable ventilation rate, the heating load is more affected by the temperature dependency than the hysteresis effect: an explanation of this difference could be based on the variations of the air flowrate between the two cases. Taking into account the hysteresis leads to a lower indoor air relative humidity, and then to lower need for air renewal which decreases the heat demands.

Conclusion

A numerical study of the hemp concrete hygrothermal behaviour at the room scale is presented. Different aspects are studied separately: the impact of the hemp concrete hysteresis as well as the influence of sorption curves temperature dependency on heat and moisture transfers and on the indoor comfort. The room is supposed to be a commercial office. For this to be done, a numerical model based on the approach of Philipe, Mendes and De Vries is created and implemented in SPARK simulation tool (Model#1). It is completed by the hysteresis model based on Pedersen approach (Model#2) and by Poyet's model for temperature dependency (Model#3). After being validated at the wall scale, the numerical models are applied at the room scale. Two ventilation strategies are studied: constant and relative humidity sensitive ventilation rate. The results of the three models are close in terms of indoor air temperature and relative humidity: air temperature is not affected by the model's type but respects the conditions of the PI controller. Taking into account the hysteresis seems to improve indoor comfort with a lower relative humidity. On the contrary, the model with temperature dependency gives high indoor relative humidity. In terms of energy consumption, the heating demands decrease with the relative humidity dependent flowrate. They are the highest for the model with temperature dependency in both ventilation strategies: constant and variable airflow rate. The cooling loads are the lowest in both cases when taking into account the variations of the sorption isotherms with temperature. An

analysis of the thermal conductivity of the hemp concrete in each case, as well as the air flowrate ventilation variations could provide satisfactory explanation for these results.

A global model which accounts simultaneously for hysteresis and temperature dependency is under development right now. It will permit to have greater understanding of physical phenomena and interpret more the results. As general conclusion, the three models could predict in a satisfactory way the hygrothermal behaviour of the hemp concrete at the room scale since the comparison does not reveal large differences in the results. For some facilities like numerical simplifications and time solving reduction, standard model of heat and moisture transfers could be very reliable at the room scale.

Nomenclature

Table 7: List of symbols

Symbol	Definition
C_p	Specific heat at constant pressure [J.kg^{-1}.K^{-1}]
C_{p_0}	Specific heat of dry material at constant pressure [J.kg^{-1}.K^{-1}]
C_{p_l}	Specific heat of water at constant pressure [J.kg^{-1}.K^{-1}]
h_M	Mass transfer coefficient [kg.m^{-2}.s^{-1}]
h_T	Heat transfer coefficient [W.m^{-2}.K^{-1}]
I	Thermal inertia of the room []
Le	Lewis number [-]
L_v	Latent heat of vaporization [J. kg^{-1}]
P_{v_s}	Saturated vapor pressure [Pa]
t	Time [s]
$t[d]$	Time [days]
T	Temperature [°C]
V	Volume of the room [m^3]
x	Distance into the wall [m]
θ	Volumetric moisture content [m^3.m^{-3}]
w	Moisture content [kg.kg^{-1}]
φ	Relative humidity [-]
ρ_0	Mass density of dry material [kg.m^{-3}]
ρ_a	Mass density of air [kg.m^{-3}]
ρ_l	Mass density of liquid water [kg.m^{-3}]
ρ_v	Mass density of water vapor [kg.m^{-3}]
$\emptyset$	Heat flux [W.m^{-2}]
$\emptyset_{rav}$	Radiative heat flux [W.m^{-2}]
δ_a	Permeability of the air to vapor [kg.m^{-1}.s^{-1}. Pa^{-1}]
ξ	Slope of the tangent to isothermal curves of sorption [-]
ξ_T	Slope of the tangent to non-isothermal curves of sorption [-]

References

Ait Oumeziane, Y., 2013. Evaluation des performances hygrothermiques d'une paroi par simulation numérique : application aux parois en béton de chanvre.Thèse de Doctorat. INSA de Rennes.

Aït Oumeziane, Y. et al., 2016. Influence of temperature on sorption process in hemp concrete. *Construction and Building Materials*, 106, pp.600–607.

Asdrubali, F., D'Alessandro, F. & Schiavoni, S., 2015. A review of unconventional sustainable building insulation materials. *Sustainable Materials and Technologies*, 4, pp.1–17.

Burch W.C and Thomas D.M, 1991. *An analysis of moisture accumulation in a wood frame wall subjected to winter climate*, National Institute of Standards and Technololgy.

Cerezo, V., 2005. *Propriétés mécaniques, thermiques et acoustiques d'un matériau à base de particules végétales : approche expérimentale et modélisation théorique*. Institut National des Sciences Appliquées de Lyon, Ecole Nationale des Travaux Publics de l'Etat.

Colinart, T., Lelievre, D. & Glouannec, P., 2016. Experimental and numerical analysis of the transient hygrothermal behavior of multilayered hemp concrete wall. *Energy and Buildings*, 112, pp.1–11.

Collet, F., 2004. *Caractérisation hydrique et thermique de matériaux de génie civil à faibles impacts enivoronnementaux*. Instittut National des Sciences Appliquées de Rennes.

Collet, F. et al., 2008. Porous structure and water vapour sorption of hemp-based materials. *Construction and Building Materials*, 22(6), pp.1271–1280.

Crausse, P., Laurent, J.. & Perrin, B., 1996. Influence des phénomènes d'hystérésis sur les propriétés hydriques de matériaux poreux: Comparaison de deux modèles de simulation du comportement thermohydrique de parois de bâtiment. *Revue Générale de Thermique*, 35(410), pp.95–106.

D'Alessandro, F., Asdrubali, F. & Baldinelli, G., 2014. Multi-parametric characterization of a sustainable lightweight concrete containing polymers derived from electric wires. *Construction and Building Materials*, 68, pp.277–284.

Elfordy, S. et al., 2008. Mechanical and thermal properties of lime and hemp concrete ("hempcrete") manufactured by a projection process. *Construction and Building Materials*, 22(10), pp.2116–2123.

Johannesson, B. & Janz, M., 2009. A two-phase moisture transport model accounting for sorption hysteresis in layered porous building constructions. *Building and Environment*, 44(6), pp.1285–1294.

Keresteciogl u A. and Gu L., 1989. *Incorporation of the effective penetration depth theory into TRNSYS*, Draft Report, Florida Solar Energy Center, Cape Canaveral, FL.

Kool, J.B. & Parker, J.C., 1987. Development and evaluation of closed-form expressions for hysteretic soil hydraulic properties. *Water Resources Research*, 23(1), pp.105–114.

Künzel Hartwig, M., 1995. *Simultaneous Heat and Moisture Transport in Building Components: One and two dimentional calculation using simple parameters*, suttgart.

Le, A.D.T. et al., 2015. Effect of Temperature-dependent Sorption Characteristics on The Hygrothermal Behavior of Hemp Concrete. *Energy Procedia*, 78, pp.1449–1454.

Lelievre, D., 2015. *Simulation numérique des transferts de chaleur et d'humidité dans une paroi multicouche de bâtiment en matériaux biosourcés*. Université Bretagne-Sud.

Lelievre, D., Colinart, T. & Glouannec, P., 2014. Hygrothermal behavior of bio-based building materials including hysteresis effects: Experimental and numerical analyses. *Energy and Buildings*, 84, pp.617–627.

Maděra, J. et al., 2012. Effect of hysteresis on moisture transport in porous building materials. In AIP Publishing, pp. 2062–2065.

Mendes, N. et al., 1999. Umidus: a PC Program For The Prediction Of Heat And Mass Transfer In Porous Building Elements. In Kyoto: International Conference on Building Performance Simulation (IPBSA 1999).

Milly, P.C.D., 1982. Moisture and heat transport in hysteretic, inhomogeneous porous media: A matric head-based formulation and a numerical model. *Water Resources Research*, 18(3), pp.489–498.

Mualem, Y., 1974. A conceptual model of hysteresis. *Water Resources Research*, 10(3), pp.514–520.

Noël, J. & Roux, J.-J., 2004. CoDyBa -Manuel Utilisateur CoDyBA Manuel Utilisateur Nouveautés de la version 6.4 de CoDyBa.

Ozaki, A. et al., 2001. Systematic analysis on combined heat and water transfer through porous materials based on thermodynamic energy. *Energy and Buildings*, 33(4), pp.341–350..

Pedersen, C.R., 1990. Transient calculation on moisture migration using a simplified description of hysteresis in the sorption isotherms. *Proceedings of the 2nd symposion on Building Physics in the Nordic Countries*, (Technical University of Norway, Trondheim, Norway.).

Philip, J.R. & De Vries, D.A., 1957. Moisture movement in porous materials under temperature gradients. *Transactions, American Geophysical Union*, 38(2), p.222.

Poyet, S. & Charles, S., 2009. Temperature dependence of the sorption isotherms of cement-based materials: Heat of sorption and Clausius–Clapeyron formula. *Cement and Concrete Research*, 39(11), pp.1060–1067.

Rode, C. & Clorius, C.O., 2004. Modeling of Moisture Transport in Wood with Hysteresis and Temperature-Dependent Sorption Characteristics., ed. *ASHREA*. Florida.

Samri, D., 2008. Analyse physique et caractérisation hygrothermique des matériaux de construction.

Steeman, H.-J., 2009. Modelling local hygrothermal interaction between airflow and porous materials for building applications.

Tran Le, A.D., 2010. *Etude des transferts hygrothermiques dans le béton de chanvre et leur application au bâtiment*. Université de Reims-Champagne-Ardenne.

Tran Le, A.D. et al., 2010. Transient hygrothermal behaviour of a hemp concrete building envelope. *Energy and Buildings*, 42(10), pp.1797–1806.

United Nations Environment Programme (UNEP) - SBCI : http://www.unep.org/sbci/

Van Belleghem, M. et al., 2010. Sensitivity analysis of CFD coupled non-isothermal heat and moisture modelling. *Building and Environment*, 45(11 Steeman, H.-J., 2009. Modelling local hygrothermal interaction between airflow and porous materials for building applications.